J Biomol NMR (2008) 40:23–30
DOI 10.1007/s10858-007-9207-1

ARTICLE

Structure discrimination for the C-terminal domain of *Escherichia coli* trigger factor in solution

Yong Yao · Gira Bhabha · Gerard Kroon · Mindy Landes · H. Jane Dyson

Received: 19 December 2006 / Accepted: 2 October 2007 / Published online: 28 November 2007

Abstract NMR measurements can give important information on solution structure, without the necessity for a full-scale solution structure determination. The C-terminal protein binding domain of the ribosome-associated chaperone protein trigger factor is composed of non-contiguous parts of the polypeptide chain, with an interpolated prolyl isomerase domain. A construct of the C-terminal domain of *Escherichia coli* trigger factor containing residues 113–149 and 247–432, joined by a Gly-Ser-Gly-Ser linker, is well folded and gives excellent NMR spectra in solution. We have used NMR measurements on this construct, and on a longer construct that includes the prolyl isomerase domain, to distinguish between two possible structures for the C-terminal domain of trigger factor, and to assess the behavior of the trigger factor C-terminal domain in solution. Two X-ray crystal structures, of intact trigger factor from *E. coli* (Ferbitz et al., Nature 431:590–596, 2004), and of a truncated trigger factor from *Vibrio cholerae* (Ludlam et al., Proc Natl Acad Sci USA 101:13436–13441, 2004) showed significant differences in the structure of the C-terminal domain, such that the two structures could not be superimposed. We show using NMR chemical shifts and long range nuclear Overhauser effects that the secondary and tertiary structure of the *E. coli* C-terminal domain in solution is consistent with the crystal structure of the *E. coli* trigger factor and not with the *V. cholerae* protein. Given the similarity of the amino acid sequences of the *E. coli* and *V. cholerae* proteins, it appears likely that the structure of the *V. cholerae* protein has been distorted as a result of truncation of a 44-amino acid segment at the C-terminus. Analysis of residual dipolar coupling measurements shows that the overall topology of the solution structure is completely inconsistent with both structures. Dynamics analysis of the C-terminal domain using T_1, T_2 and heteronuclear NOE parameters show that the protein is overall rather flexible. These results indicate that the structure of this domain in solution resembles the X-ray crystal structure of the *E. coli* protein in secondary structure and at least some tertiary contacts, but that the overall topology differs in solution, probably due to structural fluctuation.

Keywords Chaperone · Trigger factor · C-terminal domain · Peptide binding domain · Crystal structure comparison

Introduction

The first chaperones that a newly synthesized protein chain encounters are thought to be bound to the ribosome. Trigger factor, a chaperone protein from *E. coli*, has been shown to bind to the large subunit of ribosomes with a 1:1 stoichiometry, and has been proposed as one of the first chaperones encountered by a nascent peptide. The N-terminus of a newly synthesized protein binds to trigger factor while it is still attached to the ribosome. The trigger factor–nascent protein complex subsequently dissociates from the ribosome, allowing the protein to be handed off to other cytosolic chaperones, such as the DnaK system (Hesterkamp et al. 1996; Deuerling et al. 1999; Bukau et al. 2000).

Trigger factor has a modular structure consisting of three domains, an N-terminal domain, which is the ribosome binding site (Hesterkamp et al. 1997), a central proline isomerase (PPIase) domain (Hesterkamp and

Y. Yao · G. Bhabha · G. Kroon · M. Landes · H. J. Dyson (✉)
Department of Molecular Biology, The Scripps Research Institute, 10550 North Torrey Pines Road, La Jolla, CA 92037, USA
e-mail: dyson@scripps.edu

Bukau 1996) identified initially by sequence homology with FK506-binding protein (Callebaut and Mornon 1995), and a C-terminal domain, the putative binding site for nascent peptides (Hesterkamp et al. 1997). Much work has been done to characterize the PPIase domain of trigger factor from a number of organisms. Interest has been particularly high in this domain because, for some primitive organisms, it represents the only proline isomerase activity present in the genome (Bang et al. 2000). Thus, trigger factor is thought to be one of the earliest chaperones to have evolved.

A considerable amount of structural information has been published on trigger factor domains, as well as the complete protein (Vogtherr et al. 2002; Kristensen and Gajhede 2003; Ferbitz et al. 2004; Ludlam et al. 2004). These structures are illustrated in Fig. 1. Interestingly, there are significant differences between these structures, particularly in the C-terminal peptide-binding domain (blue/cyan). The "cradle" for accommodation of the unfolded peptides, inferred from the *E. coli* trigger factor structure (Fig. 1a) is not seen in the *V. cholerae* structure (Fig. 1b). The PPIase domains of the two structures superimpose perfectly (Fig. 1c), and the ribosome-binding domains show small differences (Fig. 1d). However, the structures of the C-terminal domains (Fig. 1e and f) differ radically, to the extent that they cannot be superimposed. The crossing angle between the first two long helices (helix 2 and 3) in the C-terminal domain is different by nearly 90° (heavy helices in Fig. 1e, f), and the loop between these helices is in an entirely different position, in close proximity to and facing the ribosome binding domain in the *E. coli* structure (Fig. 1a) and close to the PPIase domain (away from the ribosome binding domain) in the *V. cholerae* structure (Fig. 1b). The differences in the two C-terminal domain structures should give rise to characteristic features in NMR spectra, without the necessity for a time-consuming full-scale solution structure calculation. Questions that can be resolved in such a study include: Is

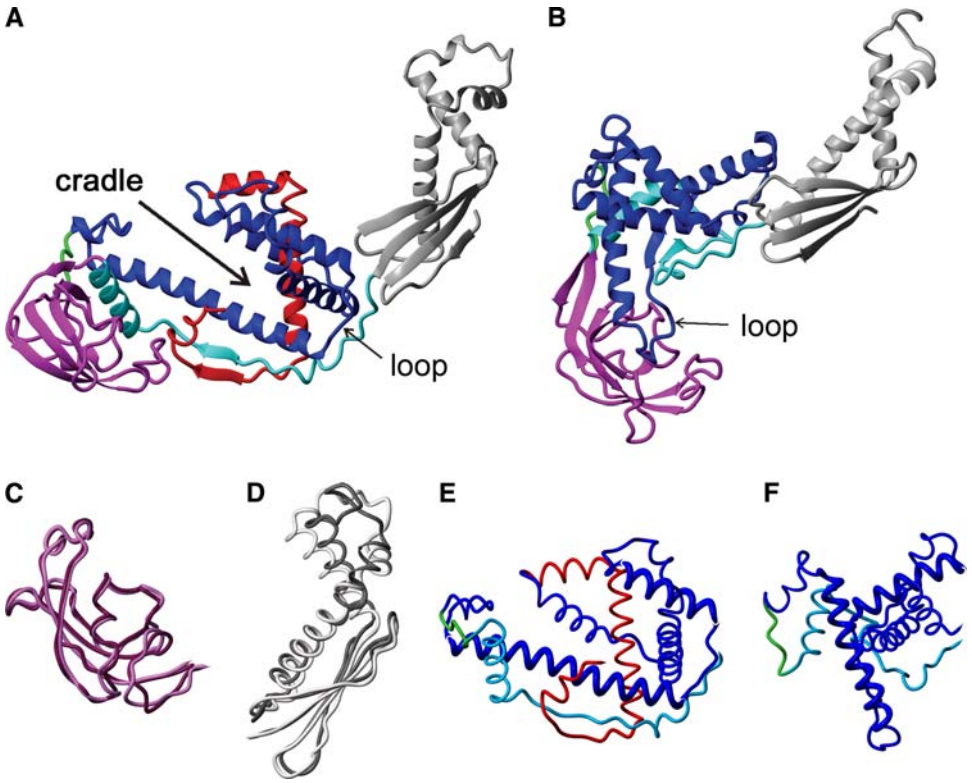

Fig. 1 (**a**) The structure of *E. coli* trigger factor (Ferbitz et al. 2004). (**b**) *Vibrio cholerae* trigger factor (Ludlam et al. 2004). The ribosomal binding domain (residues 1–111) is in gray, the PPIase domain (residues 151–242) is in magenta. The linker sequences between the C-terminal and PPIase domains are in green. The sequence between residues 112–148, which connects the ribosomal binding domain and the PPIase domain, and which is folded as part of the C-terminal domain, is shown in cyan. The part of the C-terminal domain common to both crystal structures (residues 250–379) is shown in blue. The part of the C-terminal domain that is missing from the *V. cholerae* structure is shown in red. The loop between helices 2 and 3 of the C-terminal domain is labeled, as is the peptide-binding "cradle" identified by Ferbitz et al. (2004). (**c**) Superposition of the PPIase domains from *E. coli* and *V. cholerae* trigger factors. (**d**) Superposition of the ribosome-binding domains from *E. coli* and *V. cholerae* trigger factors. In parts **c** and **d**, the lighter colors represent the *E. coli* and the darker colors the *V. cholerae* trigger factors. (**e**, **f**) C-terminal domains from *E. coli* and *V. cholerae* trigger factors (colors the same as part **a**). Helices 2 and 3 of the two structures are shown with thicker lines

the secondary structure consistent with the *E. coli* or *V. cholerae* structure in solution? Is the C-terminus of the protein (red in Fig. 1) necessary for the folded structure of the protein? Are the tertiary structure and interdomain contacts in solution consistent with one or other of the structures? Are the orientation of the helices consistent with the crossing angles in Fig. 1e and f? We have addressed these questions using NMR measurements of the trigger factor C-terminal domain in solution, and concluded that the trigger factor C-terminal domain shows greater consistency in secondary structure and tertiary contacts with the *E. coli* X-ray structure (Ferbitz et al. 2004) than the *V. cholerae* X-ray structure (Ludlam et al. 2004), but that the structure in solution is most probably dynamic rather than fixed in a single conformation.

Materials and methods

Protein expression and purification

The genes for TIG(113–432) and TIG(113–432Δ150–246) were cloned into a pET21a vector using standard methods. Triple $^{2}H/^{13}C/^{15}N$ labeled proteins were prepared by growing transformed *E. coli* BL21(DE3) in minimal medium in 99.99% D_2O with $^{15}NH_4Cl/(^{15}NH_4)_2SO_4$ and $^{13}C_6$-glucose as the sole nitrogen and carbon sources. Cells were grown at 37°C, induced with 1 mM IPTG at an OD_{600} of ~0.7, and induced at 15°C. Cells were harvested at an OD_{600} of ~1.8, suspended in lysis buffer (20 mM Tris pH 7.5, 150 mM NaCl and 20 mM imidazole), and lysed by sonication. The lysed cells were centrifuged and the supernatant was loaded onto a 15 ml Ni-NTA column. Protein was eluted from the column with elution buffer (20 mM Tris pH 7.5, 150 mM NaCl and 200 mM imidazole). Elutions were combined, diluted down to 35 mM NaCl and further purified through a 10 ml Q-Hi trap column with a linear gradient of buffer (20 mM Tris pH 7.5, 2 mM DTT, 1 mM EDTA and 0.6 M NaCl). The yield of purified soluble TIG(113–432) and TIG(113–432Δ150–246) in the *E. coli* expression system are about 20 mg/l culture.

NMR spectroscopy

Fractions containing TIG(113–432Δ150–246) from the Q column were combined, concentrated and dialyzed against the NMR buffer (10 mM Tris pH 6.8, 50 mm NaCl, 2 mM DTT, 1 mM EDTA). NMR samples were at a concentration of approximately 1 mM in 0.5 ml of NMR buffer containing 95% H_2O/5% D_2O. 2D ^{15}N–^{1}H TROSY (Pervushin et al. 1997), 3D TROSY-based deuterium decoupled HNCA (Salzmann et al. 1998), HN(CA)CB and 4D ^{15}N HSQC-NOESY-HSQC (Tugarinov et al. 2002) were recorded to obtain sequence specific backbone assignments. All spectra were acquired at 20°C on Bruker DRX600 with cryoprobe and AVANCE 900 spectrometers. Spectra were processed with NMRPipe (Delaglio et al. 1995), and analyzed with NMRView (Johnson and Blevins 1994). Proton chemical shifts were referenced to external DSS at 0 ppm. ^{13}C and ^{15}N chemical shifts were referenced indirectly using absolute frequency ratios.

Residual dipolar coupling measurements were acquired under the same conditions (buffer, temperature, pH) as above on the Bruker AVANCE750 spectrometer. Isotropic samples were at a concentration of approximately 0.8 mM in 0.5 ml of NMR buffer. Anisotropic samples were obtained using 8% stretched acrylamide gels (Sass et al. 2000). These gels were prepared, washed for 5 days, dehydrated at 37°C and rehydrated overnight with 0.6 ml isotropic sample. ^{15}N 2D IPAP (Wang et al. 1998) experiments were used to obtain residual dipolar couplings but, due to the size of the protein, the standard IPAP experiment gave ambiguous results, with missing anti-phase peaks and low signal/noise. Better results were obtained using standard ^{15}N HSQC (Norwood et al. 1990) and TROSY (Yang and Kay 1999) experiments, both of which gave excellent spectra. Data were processed in NMRpipe (Delaglio et al. 1995) and analyzed using NMRView (Johnson and Blevins 1994). RDCs were calculated for each cross peak from the difference of the TROSY peaks for isotropic and anisotropic media, and the RCSA, calculated from the difference of the HSQC peaks for isotropic and anisotropic media: RDC = $(\Delta\delta_{TROSY} - RCSA)*2$ (Tate et al. 2004). Theoretical RDC values of both structures were calculated using the program PALES (Zweckstetter and Bax 2000).

T_1 and T_2 relaxation measurements were obtained at 750 MHz using published pulse programs (Farrow et al. 1994). For T_1 experiments delays of 10*, 40, 80, 160, 240, 400*, 800, 1,200* and 2,000 ms were used. For T_2 experiments delays of 6*, 10, 14*, 18, 22, 34*, 42, 50, 62, 74*, 98, 122* and 162 ms were used. For the heteronuclear $[^{1}H]$–^{15}N NOE measurements (3 complete independent determinations), saturated and unsaturated spectra were recorded in an interleaved manner. Delay times with an asterisk indicate that experiments with these delay times were repeated. Data were processed using NMRpipe and analyzed using NMRView and the program Curvefit (Mandel et al. 1995).

Results

Design of C-terminal domain constructs of *E. coli* trigger factor

Both crystal structures show that the C-terminal domain of the trigger factor protein contains parts of the amino acid

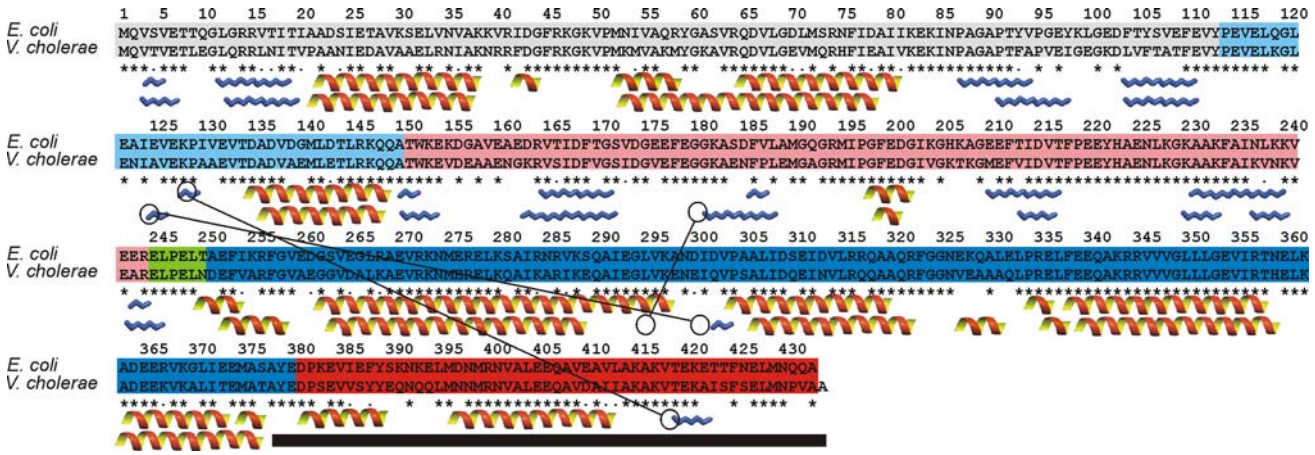

Fig. 2 Alignment of the amino acid sequences of *E. coli* and *V. cholerae* trigger factor. Colored boxes on the sequences correspond to the regions of the structure shown in Fig. 1. The final 44 residues of the *V. cholerae* sequence (no box) were not present in the construct used for crystallization (Ludlam et al. 2004). Symbols under the sequence indicate helices (red/yellow) or β-strands (blue) for the ribosome-bound *E. coli* trigger factor (Ferbitz et al. 2004) and for the free *V. cholerae* structure (Ludlam et al. 2004). The black box indicates residues missing from the *V. cholerae* structure. Small circles and lines indicate examples of close contacts inferred from coordinates of the two structures. Asterisks and dots below the sequences indicate residue identity and homology, respectively, between the two sequences

sequence that are not contiguous (Fig. 1). This is illustrated in Fig. 2, in which the sequence is colored according to the structural units shown in Fig. 1a. In order to study the solution structure of the C-terminal domain, constructs of the *E. coli* trigger factor protein were prepared corresponding to the proteins used in the two crystal structures (Ferbitz et al. 2004; Ludlam et al. 2004).

Constructs TIG(113–389) (C-terminal and PPIase domains, excluding the C-terminal 53 residues not visible in the *V. cholerae* structure) and TIG(1–389) (full-length protein, minus C-terminal residues not visible in the *V. cholerae* structure) were well expressed, soluble and well-behaved in solution, but gave poor NMR spectra, indicative of incomplete folding. We reasoned that, consistent with the *E. coli* structure, the C-terminal 43 residues might be required for structural stability. Two alternative constructs were made, TIG(113–432) and the full-length protein TIG(1–432). The full length protein gave an NMR spectrum that indicated it was aggregated (data not shown). The ^{1}H–^{15}N TROSY-HSQC spectrum of TIG(113–432) is excellent, as shown in Fig. 3a. In addition, the protein runs as a monomer on gel filtration columns, the expression yield of folded protein and the yield of pure protein are excellent, and the protein is soluble at least to 700 μM, which is outstanding for a protein of this size. However, the size of the protein is large—a total of 319 amino acids, with a molecular weight of 38 kDa—leading to inevitable overlap in some regions of the spectrum. In order to facilitate the resonance assignment process, we prepared a truncated version of the C-terminal domain, TIG(113–432Δ150–246), where the PPIase domain was excised and replaced with a short linker, with sequence Gly-Ser-Gly-Ser. This construct expressed

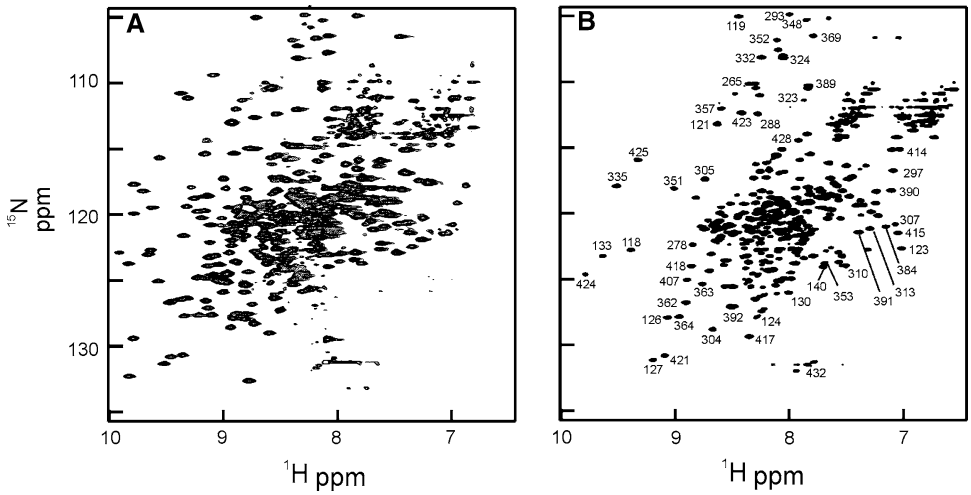

Fig. 3 (**a**) 600 MHz clean-TROSY spectrum of TIG (113–432). (**b**) 800 MHz HSQC spectrum of TIG (113–432Δ150–246), showing selected assignments

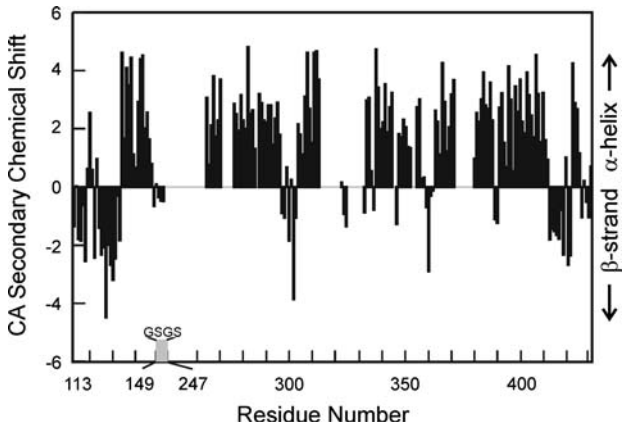

Fig. 4 Plot of secondary C^{α} chemical shifts (observed chemical shift minus sequence-corrected random coil chemical shift) versus residue number for the single-domain C-terminal construct TIG(113–432Δ150–246)

extremely well in soluble form and we were able to obtain excellent well-resolved spectra (Fig. 3b). The cross peaks in Fig. 3b can be almost exactly matched with a subset of those in the spectrum of the 2-domain construct in Fig. 3a. This observation is consistent with the idea that the domains of trigger factor are independently folded, and that there is little or no contact between the PPIase domain and the C-terminal domain, as seen in the *E. coli* structure, rather than the interdomain contact between the PPIase domain and the loop between helices 2 and 3 seen in the *V. cholerae* structure.

Resonance assignments for TIG(113–432Δ150–246)

About 80% of the backbone resonance assignments of TIG(113–432Δ150–246) were readily made using standard triple resonance techniques. The assigned residues include the complete non-contiguous region 113–149, the GSGS linker, and residues 264–269, 276–313, 322–326, 334–373 and 382–432. Consistent with both crystal structures shown in Fig. 1, the majority of the domain is helical, according to a plot of C^{α} secondary chemical shifts (Fig. 4). Two short β-strands are observed, strand 1 between residues 125 and 132 and strand 2 between 416 and 421. A total of 8 helices is observed in the set of assigned residues, mapped onto the amino acid sequence in Fig. 5, which also shows for comparison the 8 helices observed for the structure of *E. coli* trigger factor (Ferbitz et al. 2004) and the 6 helices of the structure of the *V. cholerae* trigger factor (Ludlam et al. 2004). In most cases, the helices inferred from the solution NMR chemical shifts are located in the same parts of the sequence as in both crystal structures. Significantly, the NMR studies show unequivocal evidence for well-formed helical and β-structure in the C-terminal section of the protein, which was present in the *E. coli* structure but not in the *V. cholerae* structure. An additional helix was observed by NMR at the very C-terminus, residues 426–432, the site of an irregular helix in the *E. coli* structure (see Fig. 1a).

Contacts between secondary structure elements in solution

Figure 2 shows the contacts between secondary structure elements predicted by the structures in Fig. 1a and b. The *V. cholerae* structure (Ludlam et al. 2004) predicts contacts between the PPIase domains and residues in the vicinity of 295 (helix 3) and also between the short β-strand at residues 123–125 and residues in the vicinity of 300. By contrast, for the *E. coli* structure (Ferbitz et al. 2004), contacts are predicted between the two β-strands at residues 127–129 and 418–421. Since these contacts are appreciably different, they can serve better than the simple location of secondary structural elements to distinguish between these two structures as models for the structure in solution. We observe long-range NOEs between residues in the vicinity of 128 and 420. This is illustrated in Fig. 6. These NOEs define a parallel two-strand β-sheet structure consistent with the *E. coli* crystal structure (Ferbitz et al. 2004), but not with the *V. cholerae* structure (Ludlam et al. 2004).

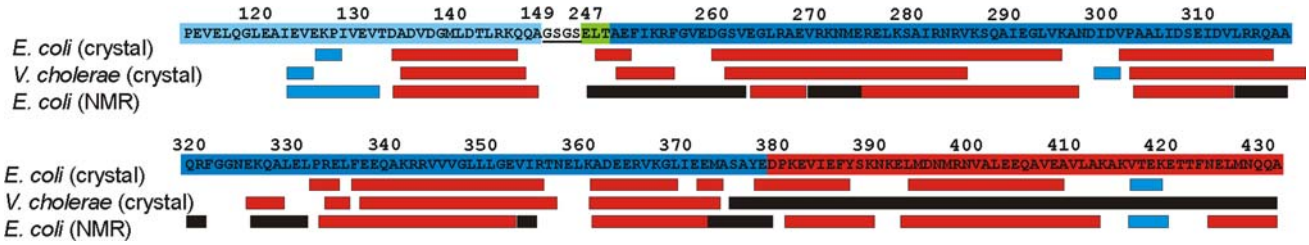

Fig. 5 Location of secondary structure observed for the TIG(113–432Δ150–246) construct. The amino acid sequence is shown outlined in boxes colored according to Figs. 1 and 2. The GSGS linker is underlined. Secondary structures obtained from NMR chemical shifts are shown in the bottom line (red: α-helix; blue: β-strand; black: resonance assignments not made). The secondary structure found in the analogous regions of the two X-ray crystal structures is shown, with red and blue indicating α-helix and β-strand, respectively, and black showing the residues absent from the *V. cholerae* X-ray structure

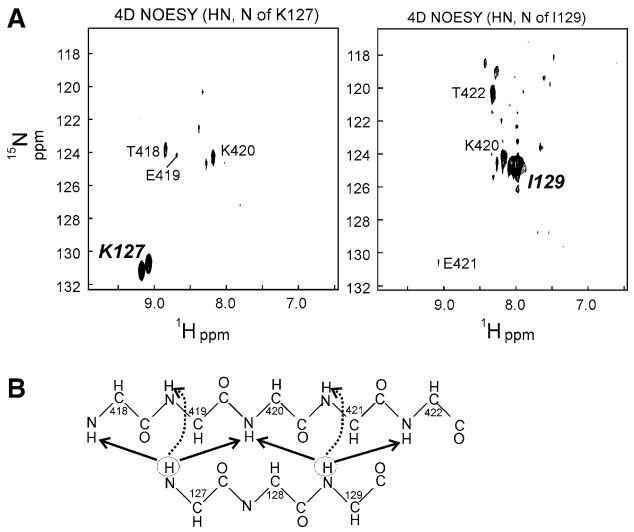

Fig. 6 (**a**) Planes from a 600 MHz 4-dimensional NOESY spectrum, showing long-range NH–NH NOEs that delineate β-sheet connectivities between residues 127–129 and 418–422. (**b**) Schematic diagram showing the connectivities mapped onto the two amino acid sequences

Residual dipolar coupling measurements

Residual dipolar couplings (RDCs) for the nitrogen-amide proton (NH) and nitrogen-carbonyl (NC) vectors were measured to obtain alignment tensors and deduce the relative orientation of the helices within the C-terminal domain. There is no correlation of the experimentally determined RDCs with theoretical couplings obtained (Zweckstetter and Bax 2000; Zweckstetter et al. 2004) for the C-terminal domain of either X-ray structure (Ludlam et al. 2004; Ferbitz et al. 2004) (data not shown). A good correlation between observed RDCs and those derived from an independently calculated structure is an indication that the (unknown) structure of the molecule giving rise to the RDCs corresponds well with the model, but a poor correlation does not necessarily indicate that the structures do not share common features (Simon et al. 2005). In addition, dynamics and flexibility can cause local averaging of RDCs to the point that correlation with structure is obscured. Taking into account trigger factor's biological role as a chaperone for many different protein molecules, we hypothesized that the poor correlation of the data for the protein-binding C-terminal domain with either crystal structure may be due to the presence of multiple different conformations in solution.

Relaxation parameters indicate flexible regions of TF C-terminal domain

In order to determine whether the lack of correlation between the measured RDC data and the two crystal structures was caused by the inherent dynamics of the molecule, we measured T_1 and T_2 relaxation parameters and heteronuclear NOEs for TIG(113–432Δ150–246). The average heteronuclear NOE is 0.68, significantly lower than expected for a well-structured protein (usually >0.8), and there are several regions that show groups of particularly low values (Fig. 7a). These include residues 130–140, 141–150 and 365–385, as well as an area of sparse data around residue 320. A loop region between residues 415–423 also shows evidence of flexibility on a ps–ns timescale, with heteronuclear NOE values of ~0.6. The values are color coded and plotted onto the *E. coli* X-ray structure, with spheres of varying radius showing the extent of motion. The T_2 parameters (Fig. 7b) indicate that motion on the μs–ms timescale is limited to a few areas that may represent points of hinge-bending in large-scale motion of subdomains of this molecule. Apart from the termini, there are five residues (149, 299, 323, 361 and 403) with above-average T_2 values. Residue 299 shows outlying values for T_1 and heteronuclear NOE as well as for T_2. Figure 7c shows that this residue forms part of a cluster of residues associated with the N-terminal non-contiguous sequence of the protein. The high amplitude and heterogeneous time scales of the motions of this region may be due to the nature of the construct used, since this is the area where the PPIase domain would normally be inserted. However, the spectra of Fig. 3 show that these two domains appear to be largely independent, with little contact in solution. The motions around residue 299 may therefore reflect phenomena that occur in the intact molecule, providing a rationale for the presence of a heterogeneous conformational ensemble in solution. Another indication of interdomain motion is the location of two of the residues with increased T_2 values at the intersection of two of the helices that cross in the *E. coli* X-ray structure. This is illustrated in the inset to Fig. 7b.

Discussion

Our results suggest that the structure of the *E. coli* C-terminal domain in solution is not consistent with the truncated *V. cholerae* crystal structure. Our evidence for this includes firstly the observed lack of a stable folded structure in solution for constructs lacking the C-terminus, whereas the constructs containing the C-terminus, both the two-domain construct TIG(113–432) and the C-terminal domain alone TIG(113–432Δ150–246) are well-folded and give NMR spectra consistent with each other. Our results indicate that the construct with the PPIase domain excised, but including the entire C-terminal sequence, shows secondary and tertiary structure that is consistent with the *E. coli* structure, but not with the *V. cholerae* structure. The RDC measurements for TIG(113–432Δ150–246) are not consistent with either X-ray structure.

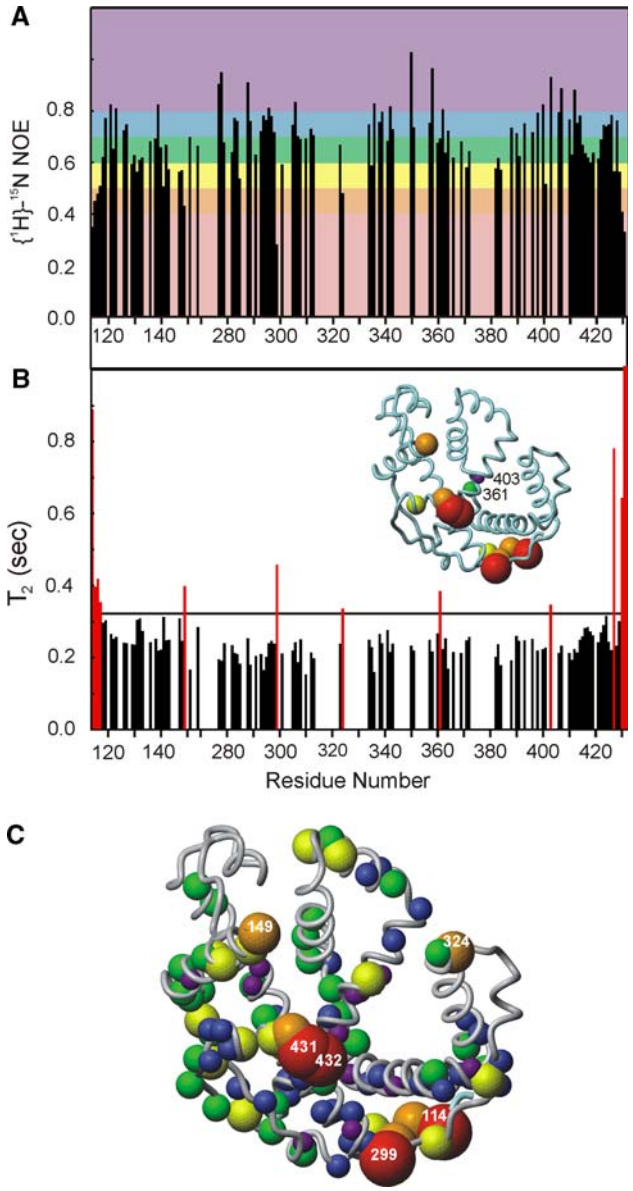

Fig. 7 (**a**) Heteronuclear [^{1}H]–^{15}N NOE values as a function of residue number. Background is shaded red (NOE < 0.4), orange (0.4 < NOE < 0.5), yellow (0.5 < NOE < 0.6), green (0.6 < NOE < 0.7), blue (0.7 < NOE < 0.8) and violet (NOE > 0.8). (**b**) Measured relaxation time T_2 as a function of residue number. Residues with values above the horizontal line at 0.33 s are designated by red bars. (Inset: Structure of the *E. coli* C-terminal domain of trigger factor {Ferbitz 2004 27321 /id} showing residues that have elevated T_2 values as a subset of the backbone nitrogens shown in part **c**). (**c**) Structure of the *E. coli* C-terminal domain of trigger factor {Ferbitz 2004 27321 /id} showing heteronuclear NOE values from part **a** mapped onto the corresponding backbone nitrogen atoms. Colors correspond to the NOE values described in part **a**, and the radius of the spheres increases in inverse proportion to the NOE value to indicate higher-amplitude motions at these sites

This is an indication that the overall topology of this domain in solution differs from that shown in the *E. coli* protein X-ray structure, or that there is conformational heterogeneity in this domain, resulting in averaged values of the RDCs.

Why are the two crystal structures of the C-terminal domain of trigger factor so different? The protein sequences are from different organisms, *E. coli* in the NMR measurements and in one of the X-ray structures, and *V. cholerae* in the second X-ray structure, but this factor should not greatly influence the three-dimensional structures, since these proteins have highly homologous amino acid sequences (Fig. 2) (71% identical, 77% homologous over the entire 432-residue sequence, 74% identical, 75% homologous in the C-terminal domain alone, and even 64% identical and 74% homologous in the C-terminal sequence that was truncated in the *V. cholerae* protein). The most likely explanation for the observed differences between the two X-ray structures is the absence of the C-terminal 44 residues that were truncated from the *V. cholerae* protein used for structure determination (Ludlam et al. 2004). We find that these residues are critical for folding of *E. coli* trigger factor into its native conformation: NMR spectra of truncated constructs indicated that they are unfolded, and a trigger factor mutant lacking the C-terminal 53 residues is functionally inactive: the truncation of these residues has been shown to result in complete loss of trigger factor chaperone activity in vitro and in vivo (Merz et al. 2006). Our results imply that this loss of function is due to improper folding and inability to adopt the correct native conformation. These observations provide an example of a case where crystallization conditions and crystal packing forces appear to have stabilized a structure that is not representative of the solution conformational ensemble of the protein.

Significantly, our residual dipolar coupling measurements do not show a good correlation even with the *E. coli* crystal structure. We initially set out to discriminate orientations of the helices in both structures using RDCs. However, our RDC data for two independent vectors is inconsistent with the *E. coli* crystal structure. From the relaxation data, we see that the C-terminal domain is quite flexible on a number of time scales, perhaps including large-scale hinge-bending motion of subdomains within the molecule, which could be responsible for the presence of a range of different orientations of the helices, even through the overall topology and structural contacts remain the same as in the *E. coli* structure.

We show in this paper that a series of simple NMR measurements can discriminate between two structures that differ in essential points. Two- and three-dimensional NMR spectra rapidly gave information on the secondary and tertiary structure that enabled us to discriminate between the two possible structures. In the case of the trigger factor C-terminal domain, which appears to be more dynamic in solution than would be suggested by either of the two crystal structures, the overall topology was not well-described by RDC measurements. RDCs would be

more appropriate in distinguishing the structures of more rigid domains.

Acknowledgements We thank Maria Martinez-Yamout for design of the deletion construct, and for many helpful discussions. This work was supported by Grant GM57374 from the National Institutes of Health.

References

Bang H, Pecht A, Raddatz G, Scior T, Solbach W, Brune K, Pahl A (2000) Prolyl isomerases in a minimal cell. Catalysis of protein folding by trigger factor from *Mycoplasma genitalium*. Eur J Biochem 267:3270–3280

Bukau B, Deuerling E, Pfund C, Craig EA (2000) Getting newly synthesized proteins into shape. Cell 101:119–122

Callebaut I, Mornon JP (1995) Trigger factor, one of the *Escherichia coli* chaperone proteins, is an original member of the FKBP family. FEBS Lett 374:211–215

Delaglio F, Grzesiek S, Vuister GW, Guang Z, Pfeifer J, Bax A (1995) NMRPipe: a multidimensional spectral processing system based on UNIX pipes. J Biomol NMR 6:277–293

Deuerling E, Schulze-Specking A, Tomoyasu T, Mogk A, Bukau B (1999) Trigger factor and DnaK cooperate in folding of newly synthesized proteins. Nature 400:693–696

Farrow NA, Muhandiram R, Singer AU, Pascal SM, Kay CM, Gish G, Shoelson SE, Pawson T, Forman-Kay JD, Kay LE (1994) Backbone dynamics of a free and a phosphopeptide-complexed Src homology 2 domain studied by ^{15}N NMR relaxation. Biochemistry 33:5984–6003

Ferbitz L, Maier T, Patzelt H, Bukau B, Deuerling E, Ban N (2004) Trigger factor in complex with the ribosome forms a molecular cradle for nascent proteins. Nature 431:590–596

Hesterkamp T, Bukau B (1996) Identification of the prolyl isomerase domain of *Escherichia coli* trigger factor. FEBS Lett 385:67–71

Hesterkamp T, Hauser S, Lutcke H, Bukau B (1996) *Escherichia coli* trigger factor is a prolyl isomerase that associates with nascent polypeptide chains. Proc Natl Acad Sci USA 93:4437–4441

Hesterkamp T, Deuerling E, Bukau B (1997) The amino-terminal 118 amino acids of *Escherichia coli* trigger factor constitute a domain that is necessary and sufficient for binding to ribosomes. J Biol Chem 272:21865–21871

Johnson BA, Blevins RA (1994) NMRView: a computer program for the visualization and analysis of NMR data. J Biomol NMR 4:604–613

Kristensen O, Gajhede M (2003) Chaperone binding at the ribosomal exit tunnel. Structure 11:1547–1556

Ludlam AV, Moore BA, Xu Z (2004) The crystal structure of ribosomal chaperone trigger factor from *Vibrio cholerae*. Proc Natl Acad Sci USA 101:13436–13441

Mandel AM, Akke M, Palmer AG (1995) Backbone dynamics of *Escherichia coli* ribonuclease HI: correlations with structure and function in an active enzyme. J Mol Biol 246:144–163

Merz F, Hoffmann A, Rutkowska A, Zachmann-Brand B, Bukau B, Deuerling E (2006) The C-terminal domain of *Escherichia coli* trigger factor represents the central module of its chaperone activity. J Biol Chem 281:31963–31971

Norwood TJ, Boyd J, Heritage JE, Soffe N, Campbell ID (1990) Comparison of techniques for ^{1}H-detected heteronuclear ^{1}H–^{15}N spectroscopy. J Magn Reson 87:488–501

Pervushin K, Riek R, Wider G, Wüthrich K (1997) Attenuated T_2 relaxation by mutual cancellation of dipole–dipole coupling and chemical shift anisotropy indicates an avenue to NMR structures of very large biological macromolecules in solution. Proc Natl Acad Sci USA 94:12366–12371

Salzmann M, Pervushin K, Wider G, Senn H, Wüthrich K (1998) TROSY in triple-resonance experiments: new perspectives for sequential NMR assignment of large proteins. Proc Natl Acad Sci USA 95:13585–13590

Sass HJ, Musco G, Stahl SJ, Wingfield PT, Grzesiek S (2000) Solution NMR of proteins within polyacrylamide gels: diffusional properties and residual alignment by mechanical stress or embedding of oriented purple membranes. J Biomol NMR 18: 303–309

Simon K, Xu J, Kim C, Skrynnikov NR (2005) Estimating the accuracy of protein structures using residual dipolar couplings. J Biomol NMR 33:83–93

Tate S, Shimahara H, Utsunomiya-Tate N (2004) Molecular-orientation analysis based on alignment-induced TROSY chemical shift changes. J Magn Reson 171:284–292

Tugarinov V, Muhandiram R, Ayed A, Kay LE (2002) Four-dimensional NMR spectroscopy of a 723-residue protein: chemical shift assignments and secondary structure of malate synthase g. J Am Chem Soc 124:10025–10035

Vogtherr M, Jacobs DM, Parac TN, Maurer M, Pahl A, Saxena K, Ruterjans H, Griesinger C, Fiebig KM (2002) NMR solution structure and dynamics of the peptidyl-prolyl cis–trans isomerase domain of the trigger factor from *Mycoplasma genitalium* compared to FK506-binding protein. J Mol Biol 318:1097–1115

Wang Y, Marquardt JL, Wingfield P, Stahl SJ, Lee-Huang S, Torchia D, Bax A (1998) Simultaneous measurement of ^{1}H–^{15}N, ^{1}H–^{13}C', and ^{15}N–^{13}C' dipolar couplings in a perdeuterated 30 kDa protein dissolved in a dilute liquid crystalline phase. J Am Chem Soc 120:7385–7386

Yang D, Kay LE (1999) Improved ^{1}HN-detected triple resonance TROSY-based experiments. J Biomol NMR 13:3–10

Zweckstetter M, Bax A (2000) Prediction of sterically induced alignment in a dilute liquid crystalline phase: aid to protein structure determination by NMR. J Am Chem Soc 122:3791–3792

Zweckstetter M, Hummer G, Bax A (2004) Prediction of charge-induced molecular alignment of biomolecules dissolved in dilute liquid-crystalline phases. Biophys J 86:3444–3460